Combining geological and historical archives to reconstruct flood variability in northwestern Italy during the last thousand years.

Giovanni Coletti[1*], giovanni.coletti@unimib.it
Laura Borromeo[1], laura.borromeo@unimib.it
Luca Fallati[1], luca.fallati@unimib.it
Marco Luppichini[2], marco.luppichini@dst.unipi.it
Agostino Meroni[1], agostino.meroni@unimib.it
Francesco Maspero[3], francesco.maspero@unimib.it
Elisa Malinverno[1], elisa.malinverno@unimib.it
Monica Bini[2], monica.bini@unipi.it
Daniela Basso[1], daniela.basso@unimib.it
Giovanni Vezzoli[1], giovanni.vezzoli@unimib.it
Eduardo Garzanti[1], eduardo.garzanti@unimib.it
Valentina Alice Bracchi[1], valentina.bracchi@unimib.it
Alessandra Savini[1], alessandra.savini@unimib.it
Fabien Desbiolles[1,4], fabien.desbiolles@unimib.it
Claudia Pasquero[1,5], claudia.pasquero@unimib.it
Annamaria Correggiari[6], anna.correggiari@bo.ismar.cnr.it
Irene Cornacchia[7], irene.cornacchia@igag.cnr.it
Chiara Boschi[8], chiara.boschi@igg.cnr.it
Ilaria Baneschi[8], i.baneschi@igg.cnr.it
Alessandro Cavallo[1], alessandro.cavallo@unimib.it
Matteo Masotta[2], matteo.masotta@unipi.it
Giulia Bosio[1], giulia.bosio@unimib.it

Andrea Gallerani[6], andrea.gallerani@ismar.cnr.it

Nicoletta Fusi[1], nicoletta.fusi@unimib.it

Luca Mariani[1], l.mariani35@campus.unimib.it

Anna Galli[3], anna.galli@unimib.it

Sergio Andò[1], sergio.ando@unimib.it

Sirio Consani[2], sirio.consani@gmail.com

Marco Lazzarotti[2], marco.lazzarotti@phd.unipi.it

Gregorio Taccola[9], gregorio.taccola@unimib.it

1: Department of Earth and Environmental Sciences, University of Milano-Bicocca, Piazza della Scienza 4, 20126 Milano, Italy.

2: Department of Earth Sciences, University of Pisa, Via S. Maria 53 - 56126 Pisa, Italy.

3: Department of Material Sciences, University of Milano-Bicocca, Via Roberto Cozzi 55, 20125, Milano, Italy.

4: CIMA Research Foundation, Via Armando Magliotto, 17100, Italy.

5: Institute of Atmospheric Sciences and Climate, Consiglio Nazionale delle Ricerche, Corso Fiume, 4, 10133, Torino, Italy.

6: Institute of Marine Sciences, Consiglio Nazionale delle Ricerche, Via Gobetti 101, 40129 Bologna, Italy.

7: Institute of Geology and Geoengineering, Consiglio Nazionale delle Ricerche, Piazzale Aldo Moro 5, 00185, Roma, Italy

8: Institute of Geosciences and Earth Resources, Consiglio Nazionale delle Ricerche, Via G. Moruzzi 1, 56124, Pisa, Italy.

9: Department of Sociology and Social Research, University of Milano-Bicocca, Via Bicocca degli Arcimboldi 8, 20126, Milano, Italy.

* corresponding author: giovanni.coletti@unimib.it

This is a non-peer reviewed preprint submitted to EarthArXiv, the manuscript has been submitted to Scientific Report on the 1/12/2023.

Abstract

Understanding Earth's changing climate is a crucial challenge. However, the available time series of direct measurements are often insufficient to fully capture climatic process that unfolds over centuries and millennia. Combining History and Geology can fill this gap. Focusing on rainfall and flood events, this research proposes a multidisciplinary approach to integrate the sedimentary and meteorological records of the Magra River (Northern Italy), using historical data as a bridge between the two datasets. A pristine record of shallow-water shelf sediments, collected at the mouth of the river and covering the last thousand years, is analysed interpreting sand layers as flood events. The results are compared with a coherent historical record of floods and river activity spanning six centuries and instrumental measurements spanning two centuries. The geological data are reasonably consistent with rainfall data and historical records, testifying for the reliability of the river mouth sedimentary record as a proxy for river discharge. The complete dataset and the comparison with other basin of the northwestern Mediterranean indicate common floods during the second half of the XII, XIV, XVI and XVIII centuries, and at the beginning of the second half of the XX century, all periods characterised by predominantly negative phases of the North Atlantic Oscillation.

Introduction

The growing awareness of the danger posed by human activities to ecosystems and the increasing demand for resources are driving environmental sciences to better constrain the complex mechanisms regulating the Earth's climate. To do so, two elements are of utmost importance: models and data to test and tune these models. However, many key environmental processes are characterized by long-term patterns (10^1-10^5 years) that instrumental data cannot fully capture since coherent measurements generally cover no more than the last 200 years. For these reasons, we must look into Earth's history, which has recorded millions of years of environmental changes. Past events are registered in the sedimentary archive, but only through indirect proxies, which imply a non-trivial level of uncertainty. Pelagic sedimentation in the deep sea may be envisaged as a slow and constant fallout of fine-grained particles, resulting in a continuous but condensed record, which proved to be fundamental in the study of glacial/interglacial cycles and climatic oscillations on the 10^3 - 10^5 year scale [e.g. Shackleton et al., 1984; Raymo et al., 1997, Barnet et al., 2019; Miller et al., 2020]. Shallow-water sedimentation is usually characterised by higher accumulation rates, making it a better tracker of climate variability on shorter time-scales, but the record is generally remarkably discontinuous [Ager, 1973]. Consequently, there is no silver bullet for tackling the challenge of tracking climatic process at the 10^2 – 10^3 years time-scale. This is however crucial for understanding rainfall patterns and their variability, which are in turn fundamental for the planning of infrastructures and for the management of the most important resource of all: water.

The current research provides a multidisciplinary approach to the problem, combining geological proxies and historical information to extract from shallow-marine sediments an archive of climatic data sufficiently accurate to be merged with instrumental data. To achieve this goal, this analysis focuses on the mouth of the Magra River (Liguria, Northern Italy), a flood-prone area with a long history of human settlements (Fig. 1). River-mouths have high rates of sedimentation suitable for recording short-term climatic processes [Macklin & Lewin, 2003]. The gap between instrumental and geological archives is bridged by the available historical documents, and the combined archives are then compared with literature data on other rivers of the northwestern Mediterranean to gain insight on climate fluctuations.

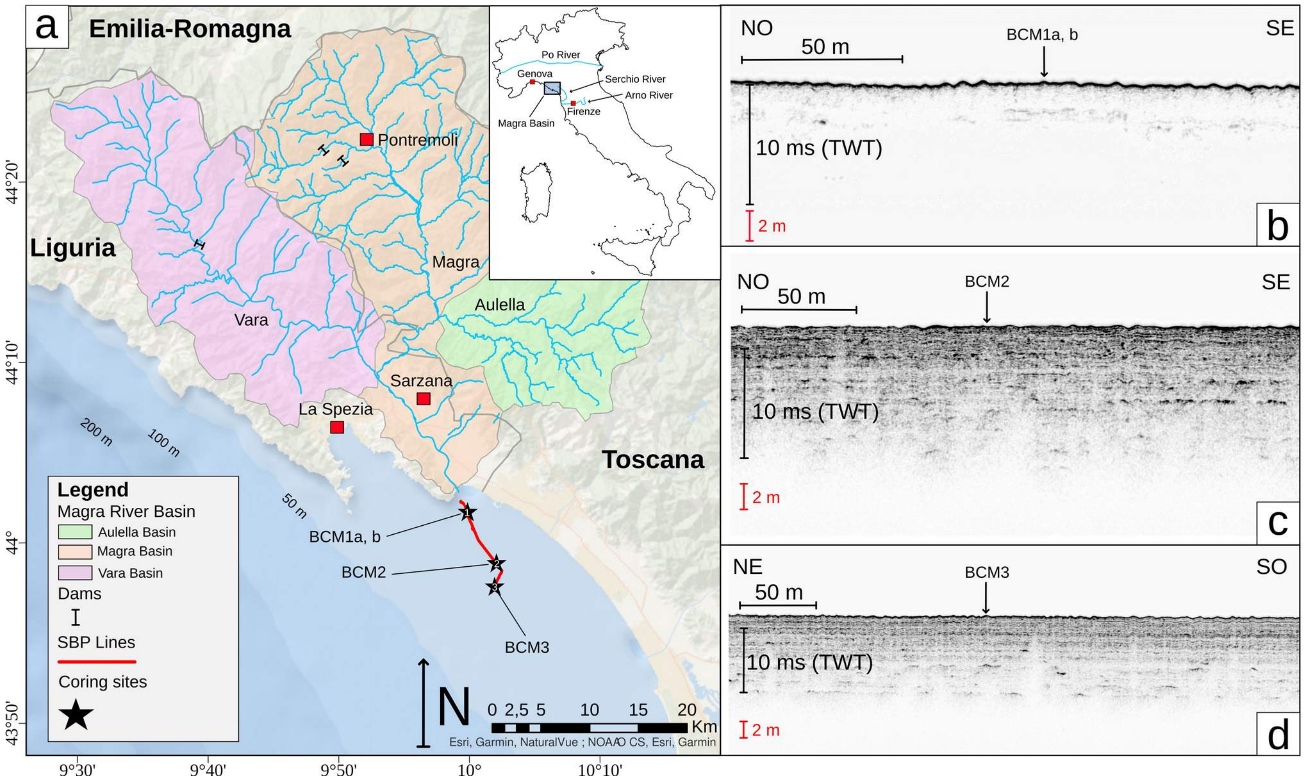

Figure 1: Study area. a) Magra River drainage basin. The main sub-basins and location of seismic lines and collected cores are indicated. Inset shows the location of the Magra Basin in northern Italy. b, c, d) Seismic sections at the location of cores BCM1a, b, BCM2, and BCM3.

Workflow, materials, and methods

The Magra River has a small catchment area [Del Bono et al., 2016; Pratellesi et al., 2018] (Fig. 1). Small basins are less complex and more sensitive to climate change than larger basins [Siriwardena et al., 2006; Bertola et al., 2020]. The area is characterized by high average rainfall and frequent storms that often lead to flood events [Rebora et al., 2013; Rinaldi et al., 2016; Brunetti et al., 2019; Luppichini et al., 2023]. The river mouth area has been significantly inhabited since Roman times [Bini et al., 2009; 2012; Raggi, 2016], providing a trove of historical data, which can be used for assessing the reliability of geological proxies [Camuffo and Enzi, 1996; Jiang et al., 2002; Calenda et al., 2005; Caporali et al., 2005; Kondrashov et al., 2005; Schmocker-Fackel and Naef, 2010; Pichard et al., 2017].

Preliminary seismic analyses were performed, using an EdgeTech SB424 sub-bottom profiler, to assess subsurface stratigraphy and select coring sites with no evidence of anthropic disturbances (e.g., sand mining). Subsequently, coring was performed with a heavy Vibrocorer deployed from a crane-equipped barge and able to collect cores 8 cm in diameter and up to 6 m in length. Four cores were collected from three different sites at different distances from the river mouth (Fig. 1a; Supplementary Material 1). Two cores (BCM1a, b), 4 and 6 m long respectively, were collected at coring site 1 (2 km offshore the river mouth). A 6-m-long core (BCM2) was collected at coring site 2, and a 5.5-m-long core (BCM3) at coring site 3 (6 and 8 km offshore the river mouth respectively). No disturbance related to coring activity occurred for the first 3 cores. The lowermost 50 cm of core BCM3 were lost during loading of the Vibrocorer on the barge. The cores were cut into 1 m-long sections, transported to Milano-Bicocca Department of Earth and Environmental Sciences, split in half and described in detail. Sixty-two samples encompassing most of the variability displayed by the sediments of the four cores were collected for laser grain-size analysis (Malvern Mastersizer 2000E™) (Supplementary Materials 2, 3). In 33 of them, bulk mineralogical characterization was assessed using X-ray diffraction (XRD) using a PANalytical X'Pert PRO PW3040/60 diffractometer (Supplementary Material 4). Among these, 11 samples were further analysed for detailed mineralogical and petrographic studies (Supplementary Material 5). The layers rich in shells or in plant remains were washed with distilled water and 16 samples resulted to contain enough carbon for ^{14}C analysis. Local reservoir correction was used for marine shells. Radiocarbon dates were calibrated using the *INTCAL20* and *Marine20* calibration curves [Heaton et al., 2020; Reimer et al. 2020] and analysed using Bayesian statistics. The age-depth models were compiled with the *Rbacon* package in *R* software [Blaauw & Christen 2011] (Supplementary Material 6). Mollusc dead assemblages were also analysed to reconstruct possible paleoenvironmental changes, with a particular focus on core BCM3.

The core was subsampled on the basis of evident changes in texture and colours. Subsamples were sieved through a 1 mm (0 Φ) mesh, and molluscs were manually picked. Identification and counting were based on [Basso and Corselli 2002, 2006]. Ecological affinity, in the framework of benthic marine bionomy [Pérès and Picard, 1964], was considered wherever possible. Species sensitivity, with respect to an increasing stress gradient (AMBI Index [Borja et al., 2000]), was also considered.

Based on radiocarbon-dating, core BCM2 was selected for further analyses. Through this core, X-ray fluorescence (XRF) analysis, performed using a third generation Avaatech Core Scanner at the Institute of Marine Sciences of Italian National Research Council (ISMAR-CNR, Bologna), allowed to obtain a continuous proxy for grain-size using Zr/Rb and Si/Al ratios (Supplementary Material 7). Both ratios correlate positively with quartz and zircon content, and hence to grain-size [Jung et al., 2014; Wu et al., 2020]. Sixty-one samples collected every 10 cm for micropaleontological studies were washed with distilled water and sieved through a 125 µm (3 Φ) mesh. Specimens of the benthic foraminifer *Ammonia tepida* were selected for inferring paleo-temperatures using the Mg/Ca ratio and the $\delta^{18}O$ of the tests as proxies [Toyofuku et al., 2011; Diz et al., 2012]. Carbon and oxygen stable isotopes were determined by a continuous-flow isotope ratio mass spectrometer (Finningan MAT Delta Plus) coupled with a GasBench II preparation device (Thermo Scientific) at the stable isotope laboratory of the Geosciences and Earth Resources Institute of the Italian National Research Council (CNR-IGG, Pisa). Each sample, which sufficient material, was analysed twice to establish the internal standard deviation. Results were reported relative to the international standard Vienna Pee Dee Belemnite (VPDB) using the international standard NBS-18 and a set of internal standards (Supplementary Material 8). The Mg/Ca ratio was determined by laser ablation-inductively coupled plasma-mass spectrometry (LA-ICP-MS) at the Center for Instrument Sharing of the University of Pisa (CISUP) (Supplementary Material 8).

Monthly rainfall data from Sarzana, Genova and Florence (Fig. 1a) for the last two decades were obtained from several institutional repositories. Older data were compiled through manual digitization of data tables from the Italian “Annali Idrologici” for the 1915-2000 period [http://www.bio.isprambiente.it/annalipdf /] and retrieved from reports of the “Ministero dei Lavori Pubblici” for the 1830-1915 period [Eredia, 1919]. Based on these data it was possible to recognize rainy periods in the region, identified as relevant excursions of the 12-month moving average above the general average (Supplementary Material 9).

Historical maps and documents from various local archives (e.g., “Archivio Familiare Fabbricotti”; “Archivio Storico del Comune di Ameglia”; “Archivio di Stato di Genova”) were used to assess the activity of the river since the year 1450. At earlier times, when the Magra’s course was not constrained by modern engineering works, the river used to significantly change its course during floods. As a consequence, land plots near the river underwent severe and repeated modifications through time. Local communities were used to hold meetings to redistribute new parcels of land formed after the floods. The analysis of these documents (“Relevaglie”) [Bonatti and Petacco, 2010] allowed to retrieve a large body of information on the major floods occurred since the year 1450 (Supplementary Material 10). Further data on historical floods were retrieved from the Atlante Climatico di Massa Carrara [Ratti, 2010], whereas information on more recent floods were collected from the SICI archives [https://sici.irpi.cnr.it/index.htm] and from the discharge data provided in the Italian “Annali Idrologici” [http://www.bio.isprambiente.it/annalipdf /] (Supplementary Material 10). The flood reports were then organized in terms of floods per decade.

Further detailed information on the different methodologies and raw data are provided and discussed in the supplementary materials (Supplementary material 1-10).

Results

Geological analysis

Seismic analysis shows that a seismic transparent substrate is overlain by 10-20 m of alternating layers of finer and coarser sediments. Close to the coast these layers are thick (Fig. 1b) and sometimes appear to be truncated or to pinch out against other layers. Offshore the layers are thinner and show a more regular parallel pattern without evidence of erosion (Fig 1c, d).

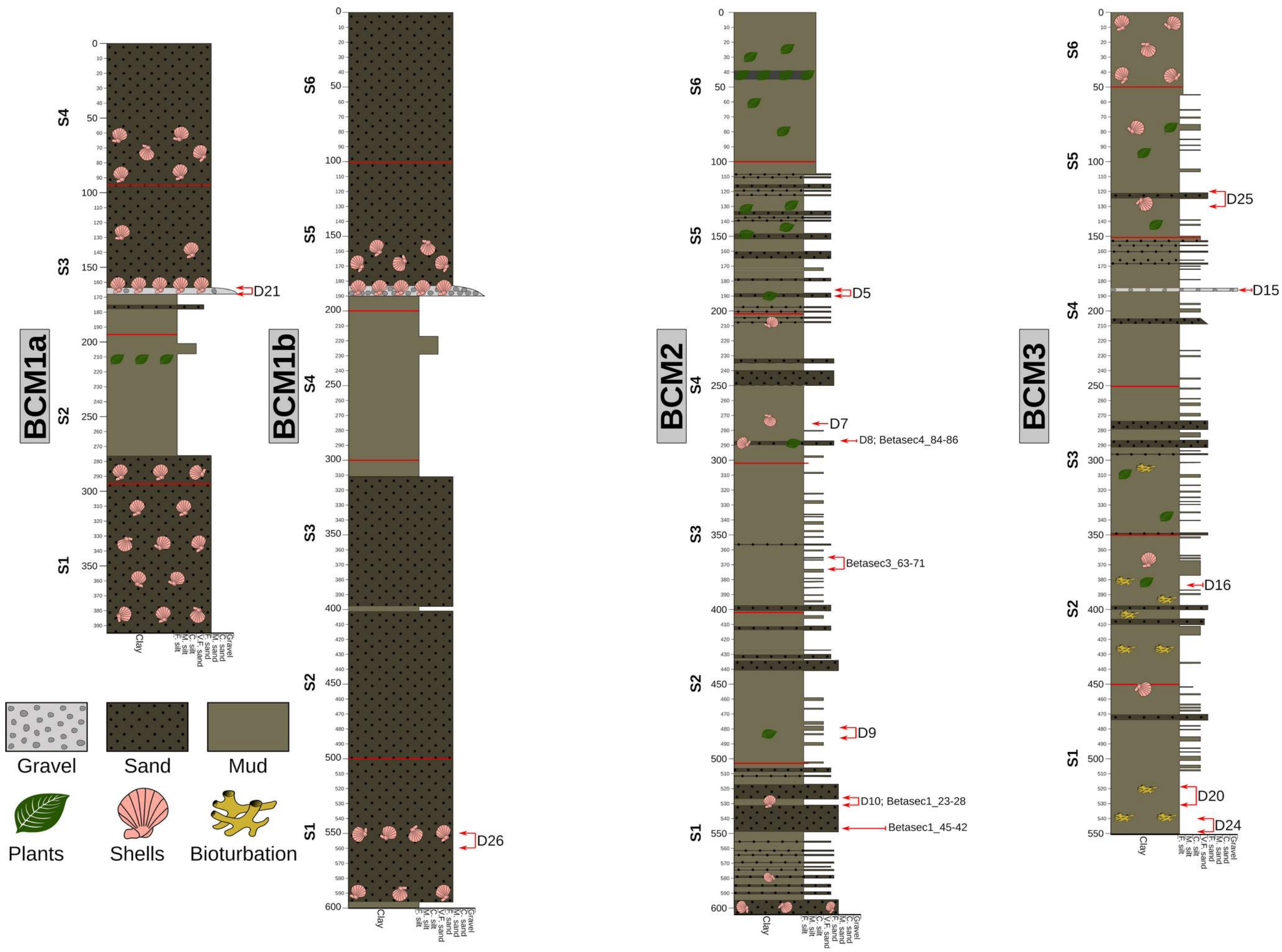

Figure 2: Stratigraphic logs of the studied cores. Identified intervals and position of samples used for radiocarbon dating are indicated, see Table 1 for further details; S= section of the core.

Cores BCM1a and BCM1b display the same stratigraphy: fine sand with scattered shells (both fragments and complete specimens) is overlain by 1 m of silt, followed by a layer rich in sub-rounded pebbles and shells capped in the topmost 2 m by fine sand with locally abundant molluscs (mainly

Nucula nucleus) (Fig. 2). The basal portion of BCM2 consists of thick layers of fine sand and thin layers of coarse silt separated by thin layers of fine silt (Fig. 2). In the overlying 2.5 m the layers of fine sand are rarer and generally thinner, whereas fine silt is more abundant (Fig. 2). The overlying 1.5 m are once again rich of layers of fine sand, whereas the uppermost 1 m consists of silt (Fig. 2). The basal portion of BCM3 consists of 0.5 m of slightly bioturbated fine silt. Upwards the core consists of 3 m of irregularly alternating layers of coarse silt (and more rarely of fine sand) and fine silt. Further above, a layer with pebbles and large-sized plant remains occurs. This layer is overlain by another 1.5 m of coarse silt and fine sand alternating with fine silt. The upper most 0.5 m consist of fine silt rich in mollusc shells.

Laser analyses indicate that the grain-size distributions of most sand layers are unimodal and poorly sorted, whereas silt layers are polymodal and very-poorly sorted. Bulk XRD highlights the presence of quartz, associated with plagioclase, K-feldspar, muscovite, chlorite, calcite, and rare dolomite. Detailed petrographic analysis indicates relevant amounts of quartz, feldspar, shale, slate and carbonate grains associated with minor serpentine grains. The poor to moderately poor transparent heavy mineral assemblages of the analysed layers are characterised by common epidote, garnet, apatite, titanite, clinopiroxene, and minor tourmaline and zircon.

Molluscs analysis focused on BCM3 highlights a relevant variety of species. The assemblage is dominated by infaunal molluscs, mainly suspension or deposit feeders, characterised by very thin and fragile shells. One third of the identified species are recognized as very sensitive to environmental stress. The whole assemblage is in agreement with the dominant size of the associated sediment. Several species are exclusively related to core intervals where mud is dominant (*Acanthocardia spinosa*, *Lembulus pella*, *Nucula nucleus*, *Spisula subtruncata*, *Thaloclamys multistriata*, *Theora lubrica*, *Varicorbula gibba*, *Cryptonatica operculata*). Other species occur in both sandy and muddy intervals (*Abra prsimatica*, *Diplodonta brocchi*, *Kellia suborbicularis*, *Litigiella glabra*, *Phaxas pellucidus*). Recognized species with ecological affinity are only *Axinulus croulinensis* (exclusive of

Coastal terrigenous muds), *Varicorbula gibba* (Heterogeneous assemblage), both occurring only at the base of BCM3, and *Kellia suborbicularis* (Coastal detritic; middle BCM3).

Core	Sample code	Depth (cm)	Material	Unmodelled calibrated calendar age (2σ)
BCM1a	D21	168-170	Bivalve shell	1912 - modern
BCM1b	D26	550-560	Bivalve shells	585 - 830
BCM2	D5	186-190	Plant remains	1670 - modern
BCM2	D7	275-276	Bivalve shell (*Nucula nucleus*)	1455 - 1820
BCM2	D8	286-288	Gastropod (*Turritella communis*)	1330 - 1615
BCM2	Betasec4_84-86	286-288	Bivalve shells (*Nucula nucleus*)	1026 - 1290
BCM2	Betasec3_63-71	365-373	Wood fragment	1120 - 1228
BCM2	D9	479-486	Plant remains	1190 - 1420
BCM2	D10	526-533	Plant remains	1305 - 1580
BCM2	Betasec1_23-28	526-533	Infaunal echinoid	829 - 1143
BCM2	Betasec1_45-42	545-548	Infaunal echinoid and bivalve shells (*Nucula nucleus*)	817 - 1132
BCM3	D25	120-130	Plant remains	1040 - 1280
BCM3	D15	185-187	Wood fragment	1760 - modern
BCM3	D16	382-385	Wood fragment	modern
BCM3	D20	519-524	Plant remains	1220 - 1475
BCM3	D24	540-550	Plant remains	1610 - 1950

Interval BCM2 (cm)	Marine model age (mean)	Marine model age (min-max)	Sedimentation rate (cm/yr)	Terrestrial model (mean)	Marine model (min max)	Sedimentation rate (cm/yr)
0-50	2021 - 1991	2021 - 1914	1.6	2021 - 1654	2021 - 1557	0.14
50-100	1991 - 1907	2021 -1825	0.59	1654 - 1552	1757 - 1463	0.49
100-150	1907 - 1822	1960 - 1735	0.59	1552 - 1450	1639 - 1366	0.49
150-200	1738 - 1822	1888 - 1648	0.59	1450 - 1350	1276 - 1514	0.5
200-250	1653 - 1738	1811 - 1562	0.59	1350 - 1265	1387 - 1201	0.43
250-300	1566 - 1653	1733 - 1471	0.57	1265 - 1179	1312 - 1125	0.58
300-350	1482 - 1566	1654 - 1376	0.59	1179 - 1093	1230 - 1052	0.58
350-400	1397 - 1482	1580 - 1281	0.59	1093 - 999	1140 - 947	0.53
400-450	1312 - 1397	1506 - 1189	0.59	999 - 900	1049 - 838	0.5
450-500	1228 - 1312	1427 - 1103	0.59	900 - 804	954 - 754	0.48
500-550	1138 - 1228	1348 - 1013	0.55	804 - 709	859 - 627	0.52
550-600	1038 - 1138	1266 - 895	0.5	709 - 608	780 -508	0.49

Table 1: Radiocarbon dating. The material used for ^{14}C analyses, its position within the core, and the resulting calibrated ages are indicated in the upper part of the table, whereas the lower part shows the result of age-depth models.

Radiocarbon dating indicates that the upper sand layer in BCM1a and BCM1b cores was deposited during the last 100 years (Table 1). Sediments underlying the pebble-rich layer are notably older, 830-585 A.D. (all the presented dates have to be intended as calendar years A.D.). Two age-depth models, one based on marine carbonate shells and the other based on plant remains, were developed for core BCM2 (Table 1). Both models indicate an average sedimentation rate of ~0.5 cm/year, a value coherent with the 0.3 – 1 cm/year range calculated for the area of the mouth of Magra River based on ^{210}Pb and ^{137}Cs analyses [Del Bono et al. 2016]. The model based on marine shells coherently suggests that the uppermost 1 m of BCM3 was deposited during the last 100 years. The model based on plant remains suggests that the uppermost 1 m of BCM3 was deposited during the last 500 years, thus strongly implying an hiatus unsupported by sedimentological observations. Plant remains may have been already decades to hundreds of years old by the time they were brought to the sea by the river and are much more prone to suspension and remobilization than shells of infaunal organisms. For these reasons, the age-model based on marine bioclasts is here considered more reliable. Among the five dated samples from core BCM3 one returned a modern age (after 1950) and four ages between 1040 and 1950, not arranged in coherent stratigraphic order (Table 1).

High-resolution studies were thus focused on core BCM2 which provided the most complete and reliable record of the sedimentation in the study area. Core-log XRF geochemical data (i.e., Zr/Rb and Si/Al proxies) display a consistent correlation with the observed grain-size distribution (Fig. 3). Paleontological analysis of the >125 μm fraction indicates that the intervals of the core with common sand layers are richer in terrigenous material and plant remains than the intervals dominated by mud, and that, overall, sand and coarse silt layers are richer in plant remains, whereas fine silt layers are richer in marine bioclasts (Fig. 3). Larger elements are mainly represented by infaunal molluscs and echinoderms associated with fish vertebrae and bryozoans. The micropaleontological assemblage is dominated by foraminifera (mainly *Ammonia tepida*, *Elphidium crispum*, *Haynesina*, miliolids and textulariids) and ostracods. *Ammonia tepida* specimens were found 59 out of 61 micropaleontological samples. Carbon and Oxygen stable isotopes analysis was carried out on the tests of *Ammonia tepida* in the 47 samples containing sufficient material. Resulting values ranged from -0.58‰ to + 1.29‰ for $\delta^{18}O$ and between -1.79‰ and -0.33‰ for $\delta^{13}C$, with a relevant number of samples (~20%) displaying a high internal standard deviation (>0.3‰) (Fig. 3). The Mg/Ca ratio could be reliably assessed in 47 samples and the resulting values are comprised between 0.30 and 1.09 mmol/mol.

Figure 3: Stratigraphy of the BCM2 core. Zr/Rb and Si/Al ratios were determined by XRF; $\delta^{18}O$, $\delta^{13}C$, and Mg/Ca ratio (determined by LA-ICP-MS) were measured on Ammonia tepida tests retrieved from the >125 μm fraction of the samples; symbols are as in Fig. 2; pale blue bars in the $\delta^{18}O$ indicate the internal standard deviation of the sample; orange bars in the $\delta^{13}C$ indicate the internal standard deviation of the sample.→

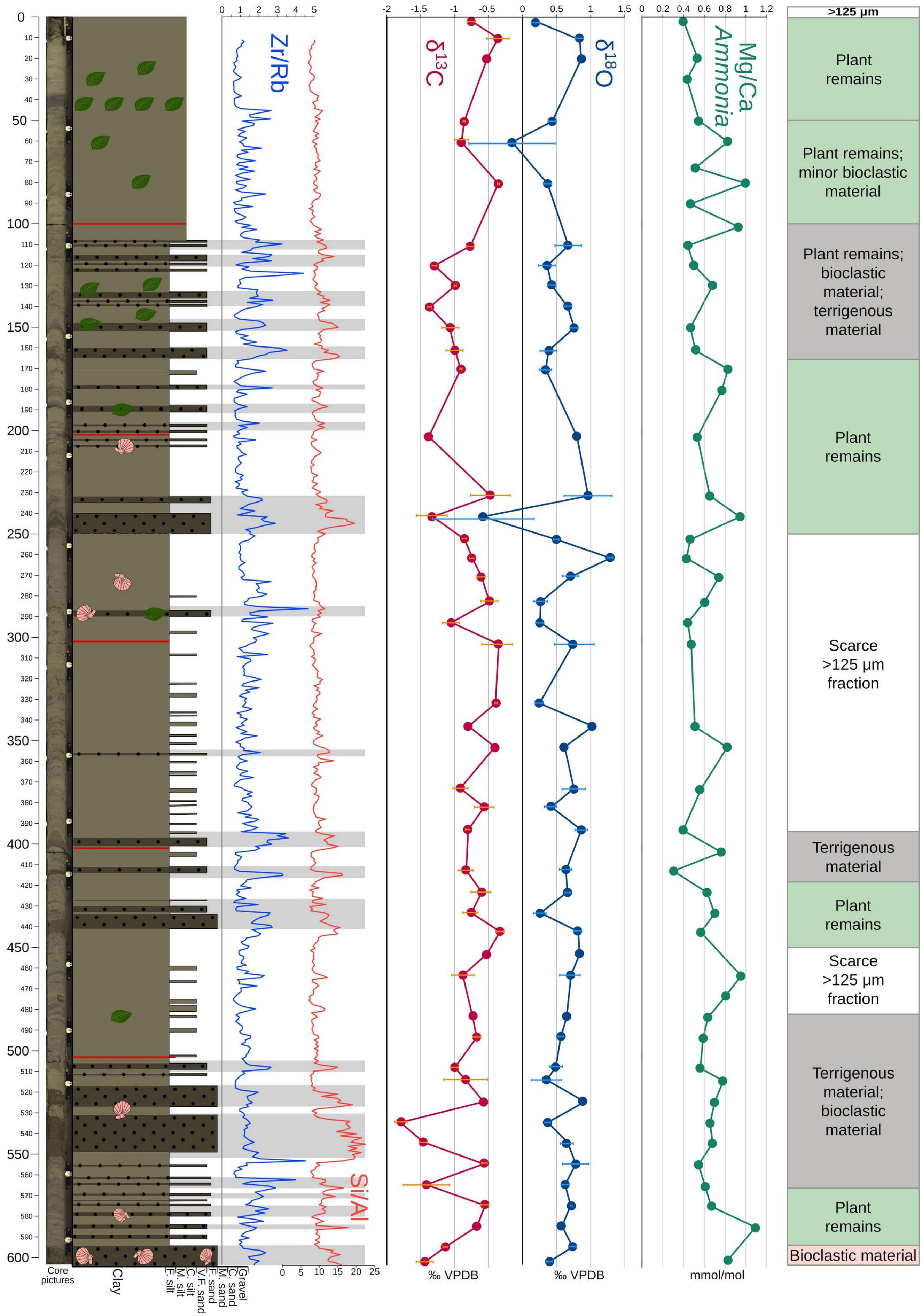
Core pictures
Clay
F. silt
M. silt
C. silt
V.F. sand
F. sand
M. sand
C. sand
Gravel
Zr/Rb
Si/Al
δ13C
‰ VPDB
δ18O
‰ VPDB
Mg/Ca Ammonia
mmol/mol
>125 µm
Plant remains
Plant remains; minor bioclastic material
Plant remains; bioclastic material; terrigenous material
Plant remains
Scarce >125 µm fraction
Terrigenous material
Plant remains
Scarce >125 µm fraction
Terrigenous material; bioclastic material
Plant remains
Bioclastic material

Rainfall and historical analyses

Monthly rainfall data of the study area allowed us to identify several rainy periods (higher rainfall than the long-term average) between 1832 and 2022 (Fig. 4a). In this time span, ~60% of recorded flood events fall within the identified rainy periods. Historical reports of floods between 1450 and 2000 indicate that nearly 60% of recorded floods occur in Autumn, with nearly one out of three floods taking place between the 20th of October and the 10th of November. Before year 1900, strong flood activity is recorded in the 1550-1590, 1720-1820, and 1880-1890 intervals (Fig. 4b), whereas fewer floods occurred in the 1470-1490, 1590-1700, and 1840-1860 intervals (Fig. 4b). After the year 1900 flood reports becomes more common and indicate that flood activity was high in the 1950-1960 and 1990-2000 intervals and low in the 1910-1920 interval. Reduced flood activity (in comparison to the intervals before and after) is also recorded between 1980 and 1990 (Fig. 4b).

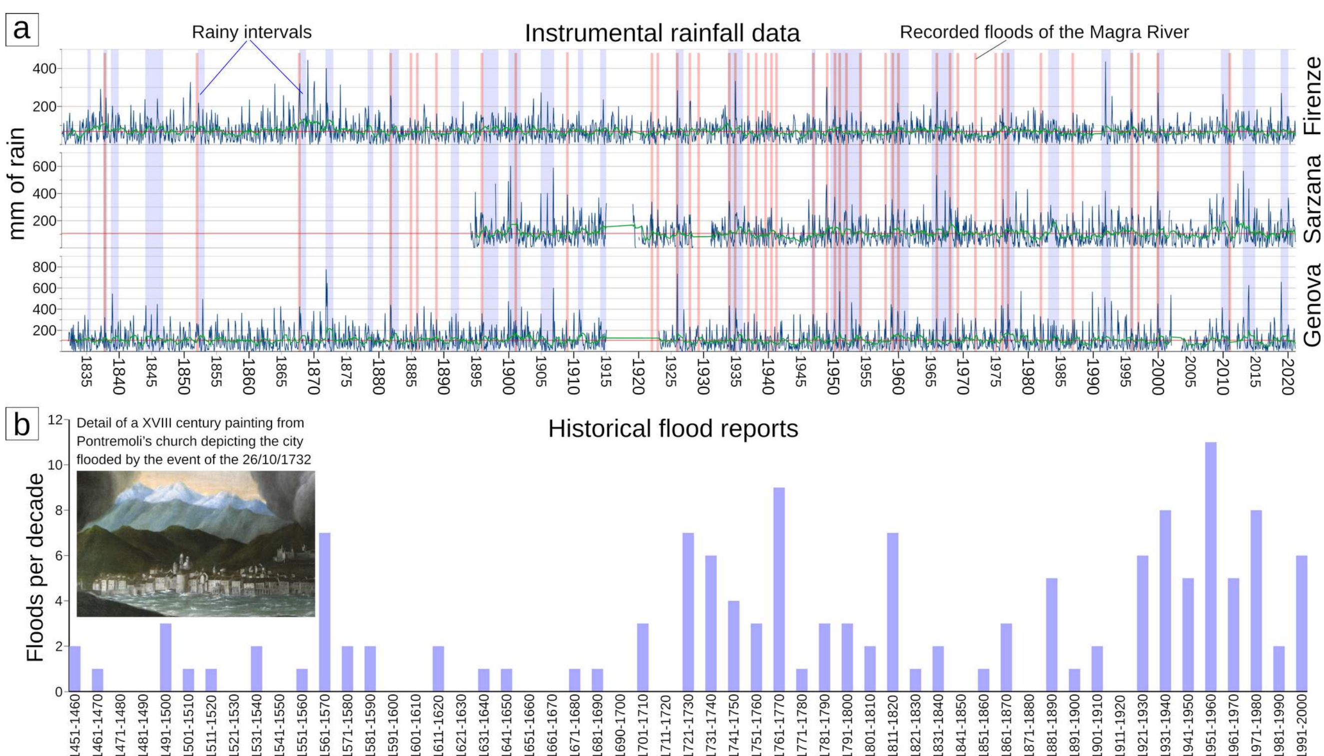

Figure 4: Meteorological and historical data. a) Monthly rainfall data from northern Tuscany (Firenze), study area (Sarzana), and Liguria (Genova) (Fig 1a). Red horizontal line represents the long-term average, the green curve the 12-month moving average, the red vertical lines the recorded Magra River floods between years 1830 and 2011. b) Historical flood record between years 1450 and 2000 with a detail of one of the sources recording the devastating flood of 26/10/1732.

Historical maps and reconstructions show that the shoreline steadily advanced from Roman times until around the year 1900, followed by shoreline retreat and erosion. Around the beginning of the XX century, all salt marshes and wetlands had been reclaimed and a steep increase in urbanization rate occurred in the Magra Basin. Industrial sand-mining activities at the mouth of the river also started. Finally, between 1930 and 1940, three dams were built in the Magra catchment, one along the Vara River and two along the Magra River (Fig. 1a).

Discussion

Monthly rainfall data indicate that, during the XIX and XX century, most rainy periods and flood events (~75%) correspond or are closely associated to negative phases of the winter North Atlantic Oscillation (NAO) (Fig. 5a). The NAO index is calculated as the difference in atmospheric pressure over the Atlantic Ocean between higher (e.g, Iceland) and lower latitudes (e.g, Azores Islands), and it is known to be inversely related to rainfall intensity in the study area [Hurrell, 1995; Luppichini et al., 2021, 2022]. Data on both rainfall and floods are available for the XIX and XX centuries (Fig. 5). For earlier periods only historical reports of floods are available (Fig. 5b). The consistency of the rainfall dataset and the historical floods dataset during the XIX and XX centuries testify in favor of the reliability of the historical flood dataset. The comparison of the flood historical record of the Magra with those of the nearby Arno and Serchio rivers (Fig. 1a) highlights similar patterns, with common floods identified in the 1550-1590 and 1720-1820 intervals, and scarce floods in the 1470-1490 and 1600-1700 intervals [Caporali et al., 2005, Nardi, 2010]. Historical floods analysis carried out on Swiss catchments highlights flood-rich periods (1561-1590, 1741-1790, 1811-1940 peaking in the 1881-1890 decade, and 1971-2007) and flood-poor periods (1500-1560, 1591-1740, 1791-1810, 1941-1970) [Schmocker-Fackel and Naef, 2010]. Consistent patterns are also shown by the lower Rhône valley record, documenting more intense flood activity in the 1450-1580, 1690-1710, 1750-1850 and 1900-2000 intervals than between 1600 and 1690. Both the 1550-1590 and 1720-1820 intervals, when the Magra and other rivers were frequently in flood, are periods of mainly negative NAO conditions reconstructed on the basis of tree-rings [Cook et al., 2019] (Fig. 5b, c). The flood-poorer period between 1590 and 1700 corresponds instead to positive or nearly positive NAO [Cook et al., 2019].

Figure 5: Correlation among rainfall events, flood events, and winter NAO. a) Comparison among winter NAO index based on instrumental data [Jones et al., 1997], identified rainy periods in the study area (Fig. 4a) and historical flood record of the Magra River; the red bars on NAO data represent positive NAO conditions; the blue bars represent negative NAO conditions; the thick black line represent the locally estimated scatterplot smoothing. b) 20-years low-pass smoothing of the winter NAO index reconstructed on the basis of proxies [Cook et al., 2019]; the red areas represent mainly positive conditions; the blue areas represent mainly positive conditions; the gray box indicates the 1450 – 2000 interval. c) Comparison among reconstructed winter NAO index [Cook et al., 2019] and historical data on Magra River floods.→

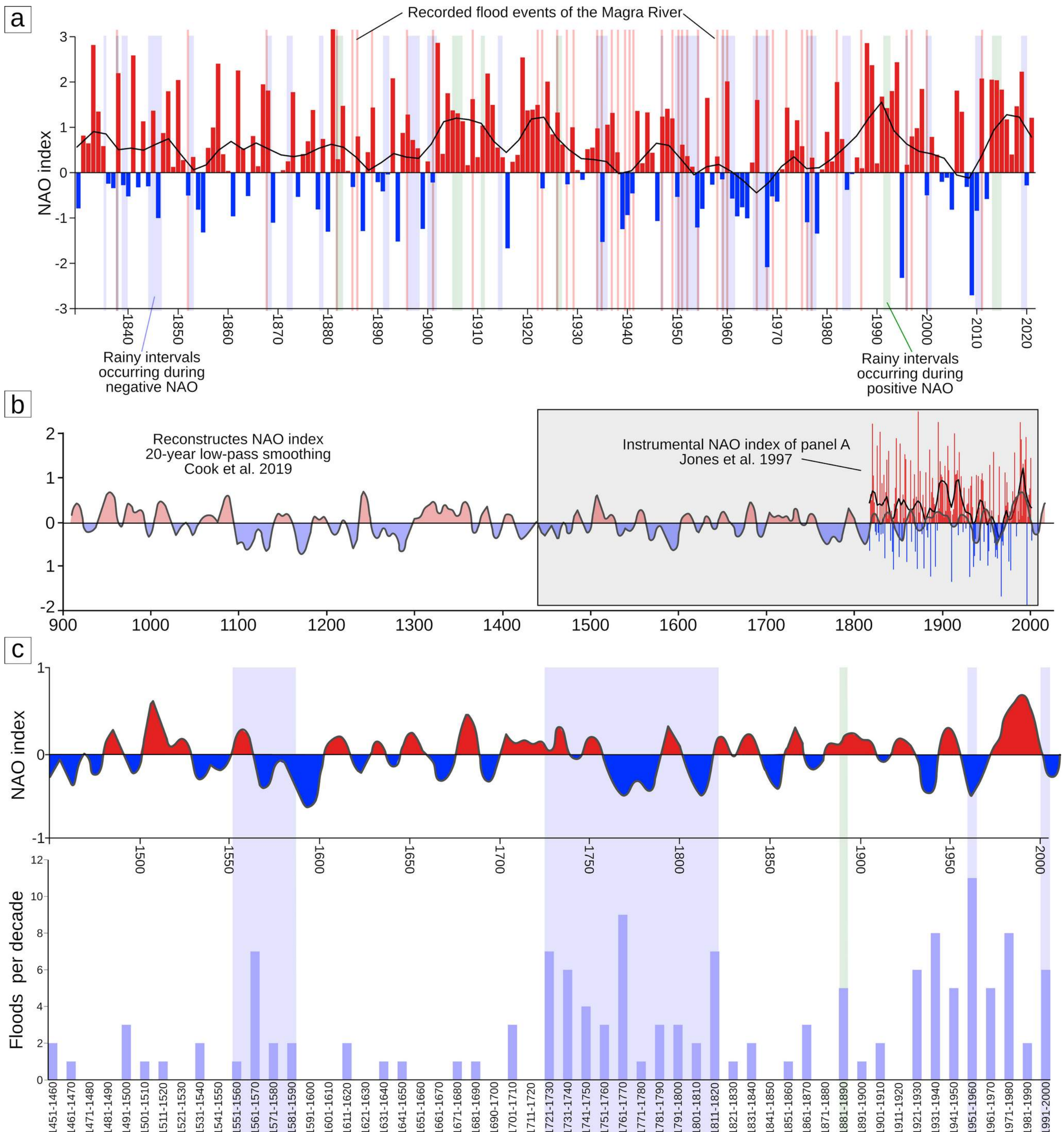

The Magra River carries quartz, feldspars, carbonate, shale, and slate grains from both remnant-ocean and foredeep turbidites, whereas serpentinite grains are supplied mostly by the Vara River draining the Inner Ligurid ophiolitic complex [Garzanti et al., 1998, 2003]. The poor to moderately poor transparent heavy-mineral assemblage is dominated by clinopyroxene associated with enstatite, minor amphibole, epidote, garnet, and rare olivine and chrome-spinel in Vara sand, and includes garnet, epidote-group minerals, clinopyroxene, minor rutile, and rare zircon and tourmaline in Magra sand [Garzanti et al., 1998, 2002]. The analysed layers of the core thus display a composition compatible with the detritus shed from the Magra Basin, consistently with provenance studies indicating that the coastal sands of northern Tuscany are largely derived from the Magra River [Garzanti et al., 1998, 2002]. The studied foraminiferal assemblages point towards a shallow-water coastal setting [Frezza et al., 2011]. Similarly, the molluscan assemblage is fully compatible with the associated sediments and does not show clear evidence of reworking. Furthermore, although radiocarbon dating of core BCM3 displays some evidence of reworking, the studied mollusc dead assemblages are coherent with the characteristics of the sediment including them. Most of identified molluscs have a benthic infaunal behavior in mud or sandy mud, and are suspension or deposit feeders, strongly implying their autochthonous nature. The presence of a consistent number of stress-sensitive species also suggests paleoenvironmental conditions that, although interested by episodic events of river transport, were not characterised by dramatic changes able to entirely replace the molluscan assemblage.

The sedimentary record of core BCM2, collected from an area unaffected by major erosion, as indicated by seismic analyses and previous geomorphological studies [Pratellesi et al. 2018], lacking notable bioturbation and major hiatuses, as suggested by sedimentological observations and radiocarbon dating, is thus considered a reasonably reliable and complete archive of Magra River activity through time. The sand layers, recognized in the core based on both sedimentology and chemical proxies (Zr/Rb and Si/Al), are usually better sorted than mud layers and are richer in terrestrial material, suggesting that they formed during flood events. Conversely, mud layers are interpreted as representing periods of limited discharge. Using the more reliable age-depth model based on marine shells, it is thus possible to constrain periods of strong activity from the Magra River (the sand layers) and compare them with rainfall data and the historical reports of floods (Fig. 6).

The sand layers between 105 and 125 cm of BCM2 core depth were deposited between 1860 and 1890. This is consistent with the 1880-1890 peak in flood activity identified from both rainfall and historical data. The underlying sand layers, between 132 and 165 cm of core depth, were deposited between 1790 and 1830, and should correspond to the last part of the flood-rich period occurred between 1720 and 1820, and possibly to the 1810-1820 flood peak. Sand layers between 170 and 200 cm of core depth, deposited between 1730 and 1770, may correspond to the central part of the 1720-1820 flood-rich period. The thick layer found between 230 and 250 cm of core depth may correspond to the strong 1732 flood event, widely reported in historical sources. However, in this instance, the correlation is less straight-forward. The mud-dominated interval between 250 and 290 cm of core depth could correspond to the 1590-1700 flood-poor period. The underlying sand layer found at 290 cm core depth and dated as 1580-1590, could be related to the 1550-1590 flood-rich period. The mud interval between 290 and 400 cm of core depth could represent the XV and most of the XVI centuries, when scarce floods characterized the Magra Basin.

The cluster of sand layers between 390 and 450 cm of core depth should have been deposited between 1340 and 1400. However, the interpretation becomes far more uncertain for layers deposited before 1450 as no coherent historical record of floods is available for the Magra Basin for events occurred before 1450. At the regional scale, in the lower Rhône valley, according to historical data, the second half of the XIV century was characterised by an increase in flood activity following a period of limited discharge [Pichard et al., 2017]. According to [Cook et al. 2019], the last part of the XIV century was characterised by a negative NAO phase, following a persistent positive NAO phase lasting for most of the XIV century (Fig. 6). The thick sand layers found at 505-550 cm of core depth may have been deposited between 1150 and 1220. Between 1152 and 1192 a catastrophic flood event is reported in the nearby lower Po valley [Andreolli, 2000]. These elements suggest a correlation with the prolonged period of sustained negative NAO that is inferred to have characterized the XII and the XIII centuries [Cook et al., 2019] (Fig. 6). The underlying thin sand layers should have been deposited between 1060 and 1100, a period characterised by mainly positive NAO [Cook et al., 2019]. The thick sand layer at the bottom of the BCM2 core, should have deposited between 1040 and 1050, and could be related to the negative NAO phase inferred for the middle XI century [Cook et al., 2019] (Fig. 6).

At beginning of the XX century, sand mining at the mouth of Magra River, together with land reclamation and engineering interventions on riverbanks, caused the disappearance of riparian habitats and salt marshes, significantly reducing the coastal deposits of sand available for erosion and transport during floods. Sand supply was further reduced by the constructions of the dams in the upper part of the Magra catchment during the 1930-1940 interval (Figs. 1a). All these elements likely contributed to the shift from advancing to retreating coastline occurred at the beginning of the XX century and recorded by various authors [Bini et al., 2009, 2012; Raggi, 2016; Pratellesi et al., 2018]. This shift is also recorded in the top 1 m of BCM2, which, coherently with the reduction of sand supply, entirely consist of silt (Fig. 6).

Overall, the dated sedimentary record of BCM2 is reasonably in agreement with rainfall data, historical data and the inferred NAO phases. Various sources of uncertainties exist, related to sedimentary processes and to the age-depth model of the core. The latter is strongly affected by the inherent limitations of ^{14}C dating of marine sediments (e.g., sediment reworking by storms, bioturbation, time-averaging, reservoir effects), suggesting that additional ^{14}C dating are unlikely to conclusively solve the existing issues. While the sedimentary record of the core provides significant data that correlate with rainfall data and historical records, the stable-isotope and Mg/Ca record based on the test of *Ammonia tepida*, does not highlight clear patterns. Our results are in line with those of *A. tepida* specimens grown at average marine salinity and temperate conditions (20 °C) [Diz et al., 2012], but they generally display a seesaw pattern suggestive that the variations in stable isotopes and chemical compositions, connected to the size of foraminiferal tests (Diz et al., 2012) and inter- and intra-test variability [Petersen et al., 2018], might have overprinted environmental variability.

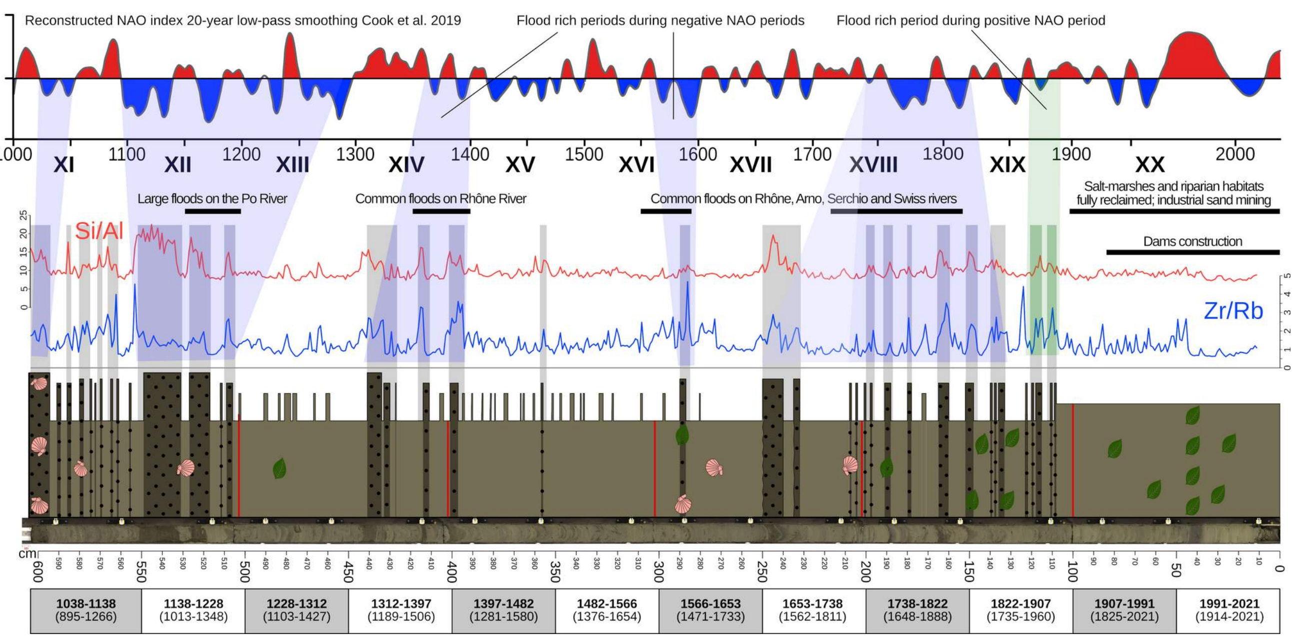

Figure 6: Comparison between the dated sedimentary record of core BCM2 and the reconstructed winter NAO index [Cook et al., 2019] for the last thousand years; the roman numbers in bold indicate the centuries; the blue overlay indicates correlation between the sedimentary record and the reconstructed NAO index; the pale blue overlay indicates possible correlation.

Concluding remarks

Meteorological and historical data on the Magra River catchment clearly indicates Autumn as the most flood-prone period of the year, with a significant number of floods occurring within a short interval of time between the end of October and the beginning of November. Both datasets suggest a close connection between rainfall, flood events, and negative phases of winter NAO. The comparison of the available historical flood record for the Magra, Arno, Serchio, Rhône and Swiss rivers indicate that floods were most frequent during the second half of the XVI and XVIII centuries and at the beginning of the second half of the XX century, whereas flood activity was limited during most of the XVII century. These correspond to periods of generally negative and positive NAO conditions, respectively. Thanks to historical information, bridging the gap between instrumental and geological data, it is possible to use the detailed shallow-marine sedimentary record retrieved from offshore the Magra River mouth as a proxy for climate variability. The sedimentary record of core BCM2 is an agreement with historical data for the XV-XIX century interval and provides information on even older periods, allowing us to highlight an intensified flood activity in the study area during the second half of the XIV century, during most of the XII an XIII centuries, and around the middle XI century. All of these are periods of reconstructed negative NAO. The comparison between the combined Magra record and other northwestern Mediterranean rivers suggests strong flood activity in the region during the second half of the XII, XIV, XVI and XVIII centuries, and during the beginning of the second half of the XX century.

Although several types of uncertainties do exist, this study indicates that the sedimentary record at river mouths might represent a reliable proxy for river discharge. Local sedimentation rates can be high enough to preserve evidence of short-lived events, resulting in a detailed record that can be tested and tuned using historical information. The approach followed in this study can offer an independent alternative to integrate and constrain data provided by established methodologies such as classical tree-ring analysis. The success of the approach is, however, strongly dependent on the availability of historical data, which provides the essential bridge between instrumental measurements and geological data.

Data Availability

Supplementary material can be accessed through this link

References

Shackleton, N.J., *et al*. Oxygen isotope calibration of the onset of ice-rafting and history of glaciation in the North Atlantic region. *Nature* **307**, 620-623 (1984).

Raymo, M.E., Oppo, D.W., & Curry, W. The mid-Pleistocene climate transition: A deep sea carbon isotopic perspective. *Paleoceanography* **12**, 546-559 (1997).

Barnet, J.S. *et al*. A high-Fidelity benthic stable isotope record of late Cretaceous–early Eocene climate change and carbon-cycling. *Paleoceanogr. Paleoclimatology* **34**, 672-691 (2019).

Miller, K.G. *et al*. Cenozoic sea-level and cryospheric evolution from deep-sea geochemical and continental margin records. *Sci. Adv*. **6**, eaaz1346; DOI: 10.1126/sciadv.aaz1346 (2020).

Ager, D.V. The nature of the stratigraphical record. (Wiley & Sons 1973).

Macklin, M.G., & Lewin, J. River sediments, great floods and centennial-scale Holocene climate change. *J.Quat.Sci*. **18**, 101-105 (2003).

Delbono, I., Barsanti, M., Schirone, A., Conte, F., & Delfanti, R. ^{210}Pb mass accumulation rates in the depositional area of the Magra River (Mediterranean Sea, Italy). *Cont. Shelf Res.* **124**, 35-48 (2016).

Pratellesi, M., Ciavola, P., Ivaldi, R., Anthony, E. J., & Armaroli, C. River-mouth geomorphological changes over >130 years (1882–2014) in a small Mediterranean delta: is the Magra delta reverting to an estuary? *Mar. Geol.* **403**, 215-224 (2018).

Siriwardena, L., Finlayson, B.L., & McMahon, T.A. The impact of land use change on catchment hydrology in large catchments: The Comet River, Central Queensland, Australia. *J. Hydrol*. **326**, 199-214 (2006).

Bertola, M., Viglione, A., Lun, D., Hall, J., & Blöschl, G. (2020). Flood trends in Europe: are changes in small and big floods different? *Hydrol.Earth.Syst.Sci.* **24**, 1805-1822; doi.org/10.5194/hess-24-1805-2020 (2020).

Rebora, N. *et al*. Extreme rainfall in the Mediterranean: What can we learn from observations? *J.Hydrometeorol.* **14**, 906-922 (2013).

Rinaldi, M. *et al*. An integrated approach for investigating geomorphic response to extreme events: methodological framework and application to the October 2011 flood in the Magra River catchment, Italy. *EarthSurf.Process.Landf.* **41**, 835-846 (2016).

Brunetti, M., Bertolini, A., Soldati, M., & Maugeri, M. High-resolution analysis of 1-day extreme precipitation in a wet area centered over eastern Liguria, Italy. *Theor. Appl.Climatol*. **135**, 341-353 (2019).

Luppichini, M., Bini, M., Giannecchini, R., & Zanchetta, G. High-resolution spatial analysis of temperature influence on the rainfall regime and extreme precipitation events in north-central Italy. *Sci.Total Environ.* 880, 163368; doi.org/10.1016/j.scitotenv.2023.163368 (2023).

Bini, M., Chelli, A., Durante, A.M., Gervasini, L., & Pappalardo, M. Geoarchaeological sea-level proxies from a silted up harbour: a case study of the Roman colony of Luni (Northern Tyrrhenian Sea, Italy). Quat.Int. **206**, 147-157 (2009).

Bini, M. et al. Palaeogeographies of the Magra Valley coastal plain to constrain the location of the Roman harbour of Luna (NW Italy). *Palaeogeogr.Palaeoclimatol.Palaeoecol.* **337**, 37-51 (2012).

Raggi, G. La Bassa Val di Magra ed il sottosuolo della Piana Lunense, da Capellini ai giorni d'oggi. *Memorie della Accademia Luniganense di Scienze Giovanni Cappellini* **86**, 137-178 (2016).

Camuffo, D., & Enzi, S. The analysis of two bi-millennial series: Tiber and Po river floods in *Climatic Variations and Forcing Mechanisms of the last 2000 years* (eds. Jones, P.D., Bradley, R.S., Jouzel, J.) 433-450 (Springer Berlin Heidelberg, 1996).

Jiang, J., Mendelssohn, R., Schwing, F., & Fraedrich, K. Coherency detection of multiscale abrupt changes in historic Nile flood levels. *Geophys.Res.Lett.* **29**, 112-1 (2002).

Calenda, G., Mancini, C.P. & Volpi, E. Distribution of the extreme peak floods of the Tiber River from the XV century. *Adv.Water.Resour* **28**, 615-625 (2005).

Caporali, E., Rinaldi, M., & Casagli, N. The Arno river floods. *Giornale di Geologia Applicata* **1**, 177-192 (2005).

Kondrashov, D., Feliks, Y., & Ghil, M. Oscillatory modes of extended Nile River records (AD 622–1922). *Geophys.Res.Lett.* **32**; doi.org/10.1029/2004GL022156 (2005).

Schmocker-Fackel, P., & Naef, F. Changes in flood frequencies in Switzerland since 1500. *Hydrol.Earth.Syst.Sci.* **14**, 1581-1594 (2010).

Pichard, G., Arnaud-Fassetta, G., Moron, V., & Roucaute, E. Hydro-climatology of the Lower Rhône Valley: historical flood reconstruction (AD 1300–2000) based on documentary and instrumental sources. *Hydrol.Sci.J.* **62**, 1772-1795 (2017).

Heaton, T.J. *et al*. Marine20—the marine radiocarbon age calibration curve (0–55,000 cal BP). *Radiocarbon* **62**, 779-820 (2020).

Reimer, P. *et al*. The IntCal20 Northern Hemisphere Radiocarbon Age Calibration Curve (0–55 cal kBP). *Radiocarbon* **62**, 725-757 (2020).

Blaauw, M., Christen, J.A. Flexible paleoclimate age-depth models using an autoregressive gamma process. *BayesianAnal.* **6**, 457-474 (2011).

Basso, D. & Corselli, C. Community versus biocoenosis in multivariaye analysis of benthic molluscan thanatocoenosis. *Riv.ital.paleontol.stratigr.* **108**, 153–172 (2002)

Basso, D. & Corselli, C. Molluscan paleoecology in the reconstruction of coastal changes in *The Black Sea flood question: changes in coastline, climate, and human settlement* (eds. Yanko-Hombach, V., Gilbert, A.S., Panin, N. Dolukhanov, P.M.) 23-46 (Kluwer Academic Press, Dordrecht, 2006).

Pérès, J.M., & Picard, J. Nouveau manuel de bionomie benthique de la mer Méditerranée. (Station Marine d'Endoume 1964).

Borja, A., Franco, J. & Perez, V. A marine biotic index to establish the ecological quality of soft-bottom benthos within european estuarine and coastal environments. *Mar.Pollut.Bull*. **40**, 1100-1114 (2000).

Jung, H.S., Lim, D., Xu, Z., & Kang, J.H. Quantitative compensation of grain-size effects in elemental concentration: a Korean coastal sediments case study. *Estuar.Coast.Shelf.Sci.* **151**, 69-77 (2014).

Wu, L. *et al*. Evaluating Zr/Rb ratio from XRF scanning as an indicator of grain-size variations of glaciomarine sediments in the Southern Ocean. *Geochem.Geophys.Geosyst.* **21**, e2020GC009350; doi.org/10.1029/2020GC009350 (2020).

Toyofuku, T. *et al.* Mg/Ca and $\delta^{18}O$ in the brackish shallow-water benthic foraminifer *Ammonia* '*beccarii*'. *Mar.Micropaleontol.* **78**, 113-120 (2011).

Diz, P. *et al*. Incorporation of Mg and Sr and oxygen and carbon stable isotope fractionation in cultured *Ammonia tepida*. *Mar.Micropaleontol.* **92**, 16-28 (2012).

Annali Idrologici Storici http://www.bio.isprambiente.it/annalipdf/

Eredia, F. Osservazioni Pliviometriche raccolte a tutto l'anno 1915. Toscana e Liguria. Dal Regio Ufficio centrale di meteorologia e geodinamica. (Tipografia Nazionale Bertero 1919).

Bonatti, F., & Petacco, E. Trebiano, vicende storiche, economiche e sociali (Edizioni Giacché 2010)

Ratti, M. Atlante climatico della provincia di Massa-Carrara (Edizioni Società Metereologica Subalpina 2010)

Sistema Informativo sulle Catastrofi Idrogeologiche https://sici.irpi.cnr.it/index.htm

Hurrell, J.W. Decadal trends in the North Atlantic Oscillation: Regional temperatures and precipitation. *Science* **269**, 676-679 (1995).

Luppichini, M., Barsanti, M., Giannecchini, R., & Bini, M. Statistical relationships between large-scale circulation patterns and local-scale effects: NAO and rainfall regime in a key area of the Mediterranean basin. *Atmos.Res.* **248**, 105270; doi.org/10.1016/j.atmosres.2020.105270 (2021).

Luppichini, M., Bini, M., Barsanti, M., Giannecchini, R., & Zanchetta, G. Seasonal rainfall trends of a key Mediterranean area in relation to large-scale atmospheric circulation: How does current global change affect the rainfall regime? *J.Hydrol*. **612**, 128233; doi.org/10.1016/j.jhydrol.2022.128233 (2022).

Jones, P. D., Jónsson, T., & Wheeler, D. Extension to the North Atlantic Oscillation using early instrumental pressure observations from Gibraltar and south-west Iceland. *Int.J.Climatol.* **17**, 1433-1450 (1997).

Cook, E.R. *et al*. A Euro-Mediterranean tree-ring reconstruction of the winter NAO index since 910 CE. *Clim.Dyn*. **53**, 1567-1580 (2019).

Nardi, R. La difesa del suolo in Italia. Quaderni dell’Autorità di bacino del fiume Serchio (Stampa Menegazzo 2010).

Garzanti, E., Scutellà, M., & Vidimari, C. Provenance from ophiolites and oceanic allochtons: modern beach and river sands from Liguria and the Northern Apennines (Italy). *Ofioliti* **23**, 65-82 (1998).

Garzanti, E., Canclini, S., Foggia, F. M., & Petrella, N. Unraveling magmatic and orogenic provenance in modern sand: the back-arc side of the Apennine thrust belt, Italy. *J.Sediment.Res.* **72**, 2-17 (2002).

Frezza, V., Mateu-Vicens, G., Gaglianone, G., Baldassarre, A., & Brandano, M. Mixed carbonate-siliciclastic sediments and benthic foraminiferal assemblages from Posidonia oceanica seagrass meadows of the central Tyrrhenian continental shelf (Latium, Italy). *Ital.J.Geosci.* **130**, 352–369 (2011).

Andreolli, B. Il Po tra alto e basso Medioevo: una civiltà idraulica in *Un Po di terra* (eds. Ferrari, C., Gambi, L.) 415-443 (Edizioni Diabasis 2000).

Bini, M., Chelli, A., Durante, A. M., Gervasini, L., & Pappalardo, M. Geoarchaeological sea-level proxies from a silted up harbour: a case study of the Roman colony of Luni (Northern Tyrrhenian Sea, Italy). *Quat.Int.* **206**, 147-157 (2009).

Petersen, J., *et al.* Mn⁄Ca intra-and inter-test variability in the benthic foraminifer *Ammonia tepida*. *Biogeosciences* **15**, 331-348 (2018).

Acknowledgments

The authors gratefully acknowledge the Starting Grants program of Milano-Bicocca University aimed at funding multidisciplinary projects from young researchers and thank Ernestina Pellegrini and Roberta Rostagno for careful handling of administrative issues. Special thanks also to Andrea Gallerani (ISMAR CNR Bologna) for his support with core-log XRF analyses. This research represents a scientific contribution to Project MIUR - Dipartimenti di Eccellenza 2023-2026.

Author Contributions

G.C. (corresponding author) - Research conceptualisation and design, coordination of geological analyses, data collection, integration, analysis, interpretation, writing and editing; L.B. - Research conceptualisation and design, data collection, integration, analysis, interpretation, editing; L.F. - Research conceptualisation and design, data collection, integration, analysis, interpretation, editing; M.L. - collection of rainfall data, integration, analysis, interpretation, editing.; A.M. - analysis of rainfall data, interpretation, editing.; F.M. - collection and preparation of ^{14}C data, analysis, interpretation, writing and editing; E.M. - Research conceptualisation and design, data collection, interpretation, writing and editing; M.B. - Research conceptualisation and design, interpretation, writing and editing; D.B. - Research conceptualisation, interpretation and editing; G.V. - Petrographic data collection, analysis, interpretation, writing and editing; E.G. - Interpretation, writing and editing; V.A.B. - Data collection on mollusc fauna, integration, analysis, interpretation, writing and editing; A.S. - Research conceptualisation and design, interpretation, editing; F.D. - interpretation of rainfall data, editing; C.P. - Research conceptualisation, editing; A.Co. - Collection, analysis and integration of XRF core-log data, editing; I.C. - Research conceptualisation, collection of data on foraminiferal stable isotopes, analysis, integration, interpretation, editing; C.B. - analysis of data on foraminiferal stable isotopes, editing; I.B. - Collection, analysis and integration of data on foraminiferal stable isotopes, editing; A.Ca. - Collection, analysis and integration of bulk XRD data, editing; M.M. - Collection, analysis and integration of data on foraminiferal minor elements, writing and editing; G.B. - Collection, analysis and integration of grain-size data, editing; A.Glr. - Collection, analysis and integration of XRF core-log data, editing; N.F. - Collection of grain-size data, editing; L.M. - Collection, analysis and interpretation of data on foraminiferal assemblages, writing and editing; A.Gll. - Analysis, interpretation of ^{14}C data, writing and editing; S.A. - Interpretation and integration of data on heavy mineral assemblages, editing; S.C. - Collection, analysis and integration of data on foraminiferal minor elements, writing and editing; M.L. - Gathering and analysis of historical data on floods; editing; R.D.M. - Research conceptualisation and design, data collection; G.T. - Coordination of the activities, research conceptualisation and design, data collection, integration, analysis, interpretation, editing.

Funding

The research activities and Open Access funding have been provided by the Milano-Bicocca Starting Grants Program

Competing interests

The authors declare no competing interests.